

Optimization of a low-flip-angle phase-based 3D B1 mapping technique for high field applications

P. Storey¹, G. C. Wiggins¹, D. Santoro¹, and D. K. Sodickson¹

¹NYU School of Medicine, New York, NY, United States

Introduction: B1 mapping is important at high fields, where the RF wavelength approaches the dimensions of the human body. High fields, however, impose particular challenges, including increased SAR and larger frequency offsets in the presence of susceptibility differences and chemical shift. We have implemented a rapid 3D low-flip-angle phase-based B1 mapping technique that was originally proposed by Mugler for hyperpolarized helium applications [1], and tested in protons at 1.5T [2]. It employs a pair of composite pulses that differ only in the order of their constituent subpulses, and allows determination of the flip angle by exploiting the fact that rotations do not commute. We optimize the sensitivity and accuracy of the method for high field applications, and use it to map B1 in the legs at 3T and the brain at 7T.

Theory: The magnetization is excited using one of two composite pulses: $[\alpha(x) \alpha(y) \alpha(-x) \alpha(-y)]_n$ or $[\alpha(x) \alpha(y) \alpha(-y) \alpha(-x)]_n$ where x and y denote the axes in the rotating frame. The signal is then acquired using a gradient echo readout. For very small values of α , the pulses move the magnetization vector about a square in the transverse plane through $n + 1/2$ turns in the anticlockwise (+) or clockwise (-) direction respectively. For larger values of α , however, the magnetization does not return exactly to its starting point after each cycle (Fig 1). Depending on whether the (+) or (-) pulse is used, the final value of transverse magnetization differs by a phase, which can be detected in the emitted signal. Since the phase difference depends on the magnitude of α , it can be used to determine the effective flip angle. Fig 2 shows the phase difference $\Delta\phi = \phi_- - \phi_+$ between the clockwise and anticlockwise pulses as a function of α for various values of n , assuming that the tissue is on resonance. $\Delta\phi$ is well approximated for small values of α by $\Delta\phi \approx (n + 1/2) \alpha^2$ where α and $\Delta\phi$ are expressed in radians. From this expression it can be shown that greater gains in sensitivity to fractional B1 variations can be achieved by increasing the flip angle α of each subpulse than by using more turns. This is an important consideration when applying the technique at high fields, since the total duration of the composite pulse is limited by off-resonance effects due to imperfect shimming, susceptibility differences or chemical shift. If the magnitude of the local frequency offset is greater than $\sim 1/4\tau$, where τ is the total duration of the composite pulse, the net transverse magnetization M_\perp is substantially reduced (Fig 3a). Interestingly, however, $\Delta\phi$ is relatively flat over the range $\pm 1/2\tau$ (Fig3b). This is an important feature, since it means that the voxel size can be increased without substantially compromising the accuracy of the method. Note that while Fig 3 was plotted for $n = 1$, the general features of the pulses, including the nulls in the transverse magnetization near $\pm 1/2\tau$ and the flatness of $\Delta\phi$ within that range, hold for $n > 1$. The sensitivity of the technique is maximized by choosing $n = 1$, using the longest pulse duration possible without incurring off-resonance effects, and operating at the highest value of α within the transmit voltage and SAR limitations. The method was implemented by substituting the composite pulse for the excitation in a gradient echo sequence. Slice selection is not possible, since the required pulse durations would be too long. The sequence must therefore be applied as a 3D acquisition with sufficient partitions to cover the entire body part. Two sets of images are collected, one with the (+) pulse and one with the (-) pulse. The accuracy of the technique is improved by interleaving the pulses in alternate TR intervals, so that the same k-space line for each image set is acquired within a very short time. This avoids spurious phase offsets in the signal due to frequency drifts of the scanner. Drifts of even a few Hertz are sufficient to produce significant phase offsets over the TE period.

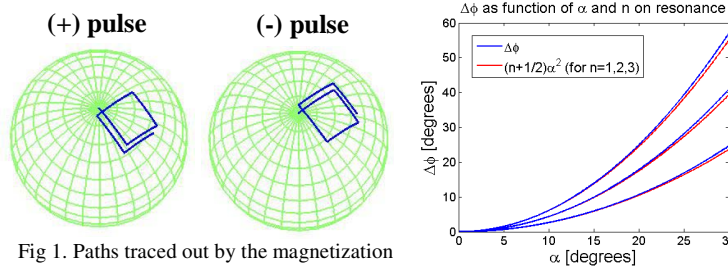


Fig 1. Paths traced out by the magnetization during the (+) and (-) pulses for $n=1$ and $\alpha=30^\circ$, assuming the magnetization starts at equilibrium (along the z axis)

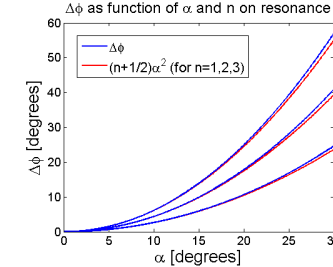


Fig 2. Phase difference between the magnetizations following the (-) and (+) pulses with the tissue on resonance, and comparison with the approximate expression $(n+1/2)\alpha^2$

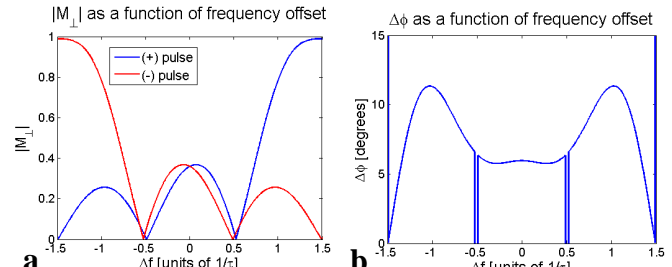


Fig 3. Amplitudes (a) and phase difference (b) of the transverse magnetizations for the (+) and (-) pulses as a function of frequency offset, for $n=1$ and $\alpha=15^\circ$

Methods: B1 mapping was performed in the thighs at 3T (4 subjects) and in the brain at 7T (3 subjects). All subjects provided informed consent under an approved IRB protocol. A composite pulse with $n = 1$, duration 450 μ s and a nominal FA ($=\sqrt{2} \alpha$) of $18 - 24^\circ$ was used. TR was 50ms at 3T and longer at 7T (up to 90ms) due to SAR limitations. The 3T studies were performed on a Siemens TIM Trio system using the integrated body coil for RF transmission and with the subject positioned feet-first supine. The resulting B1 maps were compared with simulations performed in CST Microwave Studio using a human voxel model (courtesy of Juergen Nistler). The 7T studies were conducted on a Siemens 7T whole-body scanner using an In Vivo CP head coil for RF transmission and reception.

Results: Fig. 4a shows B1 maps at three levels in the thighs at 3T. Note the rotational symmetry of the B1 profile, which decreases on the anterior medial side of the right leg and, to a lesser extent, on the posterior medial side of the left leg. The maps agree qualitatively with simulations (Fig 4b), indicating that the profile reflects an inherent feature of the interaction between a circularly polarized RF field and the human form. Fig 5 shows B1 maps in the brain at 7T. Note the maximum at the center.

Discussion: This technique offers a practical approach to 3D B1 mapping at high fields. It cannot, however, be used in 2D, and it is sensitive to the fidelity of the RF pulses. The accuracy of the method may also be slightly affected by relaxation occurring over the duration of the RF pulse.

Acknowledgements: This work was supported in part by NIH EB002568. **References:** [1] Mugler et al, ISMRM 2005, 789 [2] Mugler et al., ISMRM 2007, 351

Fig 4. (a) B1 maps of the thighs at 3T in 3 axial planes: groin (top), mid-thigh (center) and just above the knee (bottom). The color indicates the value of the effective FA divided by the nominal FA, using the scale to the right. (b) Simulated B1 profiles at similar planes, calculated in CST Microwave Studio, using a human voxel model and displayed using the same color scale.

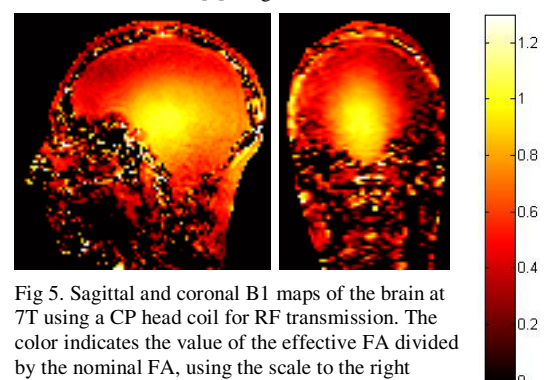
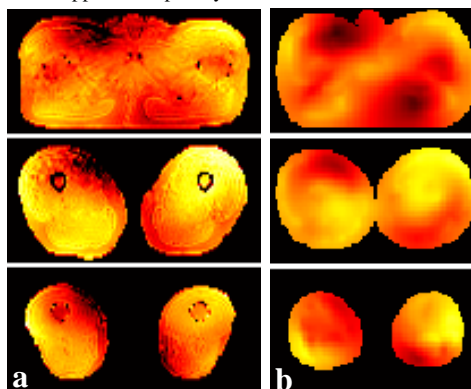


Fig 5. Sagittal and coronal B1 maps of the brain at 7T using a CP head coil for RF transmission. The color indicates the value of the effective FA divided by the nominal FA, using the scale to the right